

Spontaneous formation of geysers at only one pole on Enceladus' ice shell

Wanying Kang^{a,1} and Glenn Flierl^a

^aEarth, Atmospheric and Planetary Science Department, Massachusetts Institute of Technology

This manuscript was compiled on August 3, 2021

The ice shell on Enceladus, an icy moon of Saturn, exhibits strong asymmetry between the northern and southern hemispheres, with all known geysers concentrated over the south pole, even though the expected pattern of tidal-rotational deformation should be symmetric between the north and south poles. Using an idealized ice evolution model, we demonstrate that this asymmetry may form spontaneously, without any noticeable a priori asymmetry (such as a giant impact or a monopole structure of geological activity), in contrast to previous studies. Infinitesimal asymmetry in the ice shell thickness due to random perturbations are found to be able to grow indefinitely, ending up significantly thinning the ice shell at one of the poles, thereby allowing fracture formation there. Necessary conditions to trigger this hemispheric symmetry breaking mechanism are found analytically. A rule of thumb we find is that, for Galilean and Saturnian icy moons, the ice shell can undergo hemispheric symmetry breaking only if the mean shell thickness is around 10-30 km.

Enceladus | icy moon | planetary science

Despite its small size (252 km in radius) and hence rapid heat loss, Enceladus, an icy moon of Saturn, retains a global ocean underneath its ice shell (1, 2); geyser-like jets of water, methane, and other volatiles are shot out of the ice shell at the south pole (3–6). These unique characteristics imply a high astrobiological potential, which has triggered interest while introducing puzzles. One of the puzzles is why all these geysers, and hence most of the heat flux, are concentrated near the south pole (7–10). This puzzle is twofold: we need to understand why the geysers tend to gather to one spot, as well as why the spot is located at the south pole, knowing that the expected pattern of tidal heating is expected to be almost perfectly symmetric between the north and south hemispheres (11, 12). Previous studies have achieved the observed dichotomy by imposing an a priori anomaly in the south polar ice shell, mechanically or thermally, initially or constantly (13–16). Despite successes, these hypotheses suffer from a common issue: the origin of the asymmetry relies on either a giant impact or a monopole structure of geological activity, followed by true polar wandering (17–19), which requires some luck to form only one hot-spot, as observed.

Toward an explanation without a priori asymmetry

A concurrent work (20) proposes that the ice shell are torn apart by the overpressure induced by a secular freezing of the subsurface ocean. This occurs at poles because the ice shell is thinnest and thus weakest there; it occurs at only one of the poles because once the initial fracture forms at one pole, the overpressure would be released, preventing the same fracture from forming at the other pole.

Our work aims to propose an alternative mechanism to explain the gathering of geysers over the south pole, which does not require any significant a priori asymmetry or secular cooling. We will show that a hemispherically symmetric ice shell is not a stable equilibrium, and that hemispheric symmetry breaking could be triggered by an infinitesimal random perturbation. Two key characteristics are necessary for a symmetry-breaking mechanism: 1) it should involve some positive feedbacks that amplify the existing inhomogeneity in the ice shell and 2) it should be able to select large-scale inhomogeneities compared to small-scale ones, so that the ice shell eventually will be dominated by large-scale topography, instead of becoming “patchy” and having geysers spread all over the globe.

Overview of our ice evolution model

To understand why Enceladus ends up with a hemispherically asymmetric ice shell, we build a model to calculate how ice shell geometry would evolve. A similar problem has been looked into by (21), who analytically solved the equilibrium state of the ice shell geometry, where cooling induced by heat conduction

balances the tidal heat generation. Here, we follow a similar path, but in addition to solving for the equilibrium state, we also look into the stability of such a state.

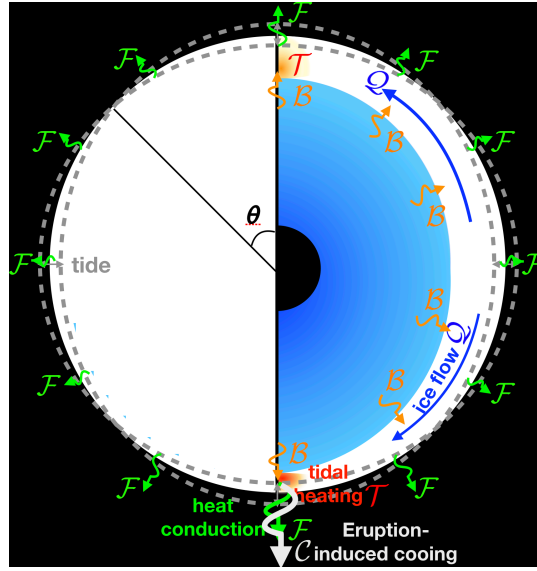


Fig. 1. Schematics to demonstrate the physics processes we consider in this model. See the main text for descriptions.

As sketched in Fig. 1, we consider a global ice sheet whose thickness profile H is simultaneously reshaped by the freezing induced by heat conduction to space \mathcal{F} (outward-pointing green curly arrows), melting induced by tidal heating \mathcal{T} (redish patches in the ice shell), mass redistribution by lateral ice flow \mathcal{Q} (blue arrows in the ice shell), crack-induced cooling \mathcal{C} , and an extra heating $\mathcal{B} > 0$. The governing equation of ice thickness evolution can be symbolically written as

$$\frac{dH}{dt} = \frac{\mathcal{F}(H) - \mathcal{T}(H)}{L_f \rho_i} + \frac{1}{a \sin \theta} \frac{\partial}{\partial \theta} (\sin \theta \mathcal{Q}(H)) - \mathcal{B}(H) + \mathcal{C}(H). \quad [1]$$

In the above equation, H denotes ice thickness, ρ_i denotes ice density, L_f denotes fusion energy, θ denotes colatitude, and a denotes the radius of Enceladus. \mathcal{F} , \mathcal{T} , \mathcal{Q} , \mathcal{B} , \mathcal{C} are all functions of the ice thickness H . Their definitions are given in the supplementary material.

The heat conduction to space \mathcal{F} is inversely proportional to H . The ice flow \mathcal{Q} flows down-gradient, smoothing the ice shell inhomogeneities, particularly those at small scales. \mathcal{Q} weakens in regions with thin ice, allowing the formation of ice “holes”. The crack-induced cooling \mathcal{C} allows extra heat loss when the ice thickness is below the crack threshold $H_{\text{crack}} = 8$ km (to account for the strong heat flux from the geysers on the south pole (7–10)). The balancing term \mathcal{B} is introduced to keep the global-mean ice thickness

Significance Statement

Enceladus, an icy moon of Saturn, is one of a handful of places where the existence of liquid water has been confirmed. Vapor emanated out of geysers over the south pole provides a unique opportunity for us to peek inside. However, why the ice shell is much thinner over the south pole than anywhere else, including the north pole, remains a mystery. Our work aims to provide an explanation for this unexpected hemispheric asymmetry. We found that, from an infinitesimal random perturbation early in the moon’s history, a significant level of asymmetry can build up over millions of years. Eventually, the ice over one of the two poles could crack open.

¹To whom correspondence should be addressed. E-mail: wanyingkang@g.harvard.edu

H_0 unchanged, as our focus here is to understand topography formation on the ice shell rather than the maintenance of the ice shell at a certain thickness.

Tidal heating generated in the ice shell and the core dominantly balances heat loss by conduction \mathcal{F} (22, 23). As Enceladus orbits Saturn, the change of geopotential induced by orbital eccentricity deforms the ice shell and the core and generates heat. Here, we focus on the tidal dissipation in the ice shell, which is sketched as two reddish patches over the poles to demonstrate the polar-amplified heating profile, as suggested by previous studies (24–27).

In a laterally varying ice shell, tidal heating \mathcal{T} would be concentrated in regions where the ice shell is thinner and thus more mobile (geometric effect), just like a rubber band with a weak point would generate more heat there. The enhanced heating rate over the thin ice regions can, in turn, warm up the ice shell, making it even more mobile (rheology feedback). To make the problem analytically approachable, we account for this effect by amplifying the membrane mode heat generation by a factor of $(H/H_0)^{p_\alpha}$. According to the calculation in (26), the geometric effect contributes -1 to p_α , and rheology feedback contributes an additional -0.6 (see supplementary material for details). Besides these, a more dissipative ice shell would have an even stronger rheology feedback (26), and ocean circulation may also contribute (see Conclusions and Discussions). Given these uncertainties, we leave p_α as a tunable parameter. The schematics depict a situation where the ice shell is thinner over the south pole and thus tidal heating is amplified there.

The idealized Maxwell rheology used here has been shown to underestimate the total tidal heat generation (28, 29). To compensate for this underestimation, a multiplicative factor, γ , is incorporated in the tidal heating formula. Since the total tidal heating in the ice shell is poorly constrained, we leave γ as a tunable parameter. Code and data used in this study can be downloaded from [here](#).

Symmetry breaking of Enceladus' ice shell

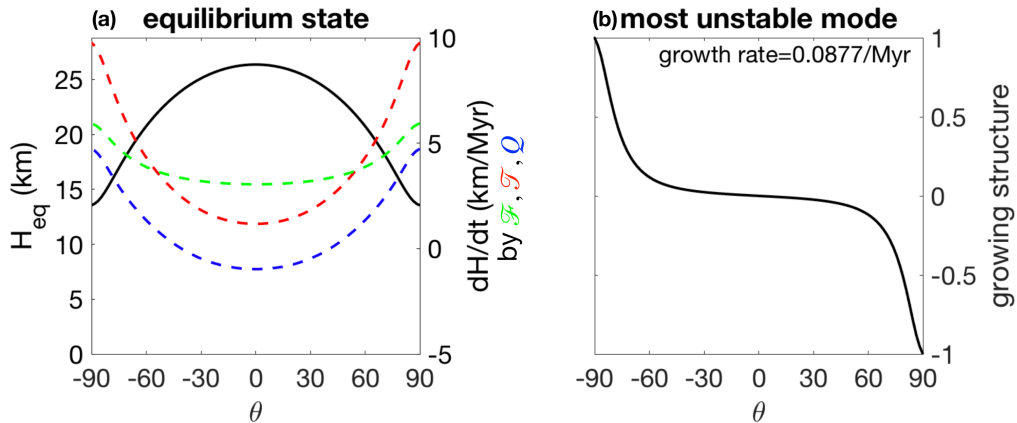


Fig. 2. The equilibrium ice thickness starting from a perfect uniform ice shell and the most unstable mode based on linear analysis. Panel (a) shows H_{eq} as a function of colatitude θ as a solid black curve with the y-axis on the left. The equilibrium-state melting/freezing rate induced by tidal heating $\mathcal{T}(H)/L_f \rho_i$ (red dashed), ice flow $\frac{1}{a} \frac{\partial}{\partial \theta} (\sin \theta Q(H))$ (blue dashed), and heat loss to space $\mathcal{F}(H)/L_f \rho_i$ (green dashed) are shown on the right axis. A minus sign is multiplied to the tidal heating curve and heat loss curve to show in the same axis. Panel (b) shows the normalized structure of the most unstable mode against colatitude θ and the corresponding growth rate.

The equilibrium ice topography H_{eq} can be obtained numerically by evolving the ice thickness model from an initial value $H(\theta) = H_0$ for a long enough period of time until the tendency terms exactly compensate each other. H_{eq} , and the corresponding melting/freezing rate induced by \mathcal{F} , \mathcal{T} , \mathcal{Q} are shown in Fig. 2a. The tidal heating \mathcal{T} peaks at the two poles. Compensated by a relatively faster heat loss to space \mathcal{F} in the polar regions and a poleward ice flow, the system reaches equilibrium, with thinner ice at the two poles. Here, we set $\gamma = 38$, which yields a 24.8 mW/m^2 tidal heating rate on global average. Since this heating rate is lower than the average heat loss rate at $\mathcal{F} = 33.8 \text{ mW/m}^2$ given by the heat conduction

* Among the three tidal dissipation modes, the membrane mode is the dominant one. Physically, it corresponds to the dissipation induced by extension/compression and tangential shearing of the ice membrane (26).

model, a positive constant balancing heating \mathcal{B} is required to keep the global ice shell thickness unchanged. Physically, this term could correspond to dissipation in the ocean or the core (23, 30, 31).

In the real world, we would not expect a perfectly uniform ice shell to begin with. If the initial ice shell thickness H is slightly and randomly perturbed around the mean H_0 , as shown by the thin dashed curve in Fig. 3, a break in symmetry between the two hemispheres appears spontaneously. After 100 million years, the ice sheet thickness reaches a final state with a significant tilting from one pole to the other, as shown by the thick solid curve in Fig. 3. This final state captures the main characteristics of ice-shell geometry constrained by observation (27, 32, 33): the ice shell is thinner at the poles than the equator, with geysers concentrated at one of the poles.

This symmetry breaking arises from a normal mode instability induced by the concentration of tidal heating in the regions where the ice shell is already thinner than elsewhere. By linearizing the ice evolution model around the unperturbed equilibrium state H_{eq} , we obtain the linear tangential system (see the last section in the supplementary material for derivation). The most unstable eigenmode structure is shown in Fig. 2b and has a pole-to-pole tilting structure. If this structure continues to grow with time, the ice shell over one of the poles (depending on the initial condition) would get thinner and thinner, and finally a parallel set of geysers may develop through the mechanism proposed in (20), as we see in Fig. 3.

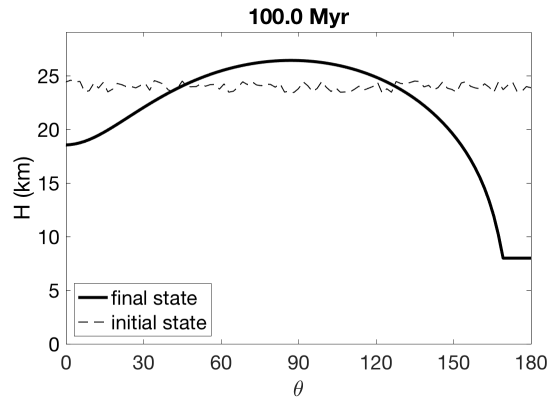


Fig. 3. The final ice topography H (thick solid curve) after evolving the ice thickness model (Eq. 1) for 100 Myr. Initial condition of H is shown as a thin dashed curve for comparison. The initial $h' = (H - H_0)/H_0$ at each grid point is independent and identically drawn from a uniform distribution between -0.025 and 0.025. The system would equilibrate faster with larger initial perturbations. p_α is set to -1.5 .

Discussions

The above calculation suggests that, without a priori asymmetry, Enceladus could naturally evolve into a state with a significant hemispheric asymmetry, and with one pole being concentrated with geysers. With the present setup ($p_\alpha = -1.5$, surface temperature $T_s = 80$ K), symmetry breaking occurs when $\gamma \in [36.9, 38.1]$, which corresponds to a global-mean ice dissipation rate of 23.8-25.1 mW/m². Below this range, the hemispheric asymmetry of the ice shell would stabilize at a hemispheric symmetric state, with no geysers anywhere. Above this range, the topography self-amplification becomes so strong that not only the degree-1 mode but also the degree-2 mode would become unstable. The degree-2 mode could dominate over degree-1 because the polar-amplified tidal heating profile would force a degree-2 pattern in H_{eq} , even without perturbations. As a result, geysers (ice thinner than 8 km) would form in both poles. Symmetry breaking occurs within a relatively narrow range of γ for most of the parameters we explore here because γ needs to be large enough for the degree-1 mode to grow while small enough for other modes (in particular degree-2 mode) to decay.

To show that the symmetry-breaking mechanism is not completely sensitive to the choice of poorly constrained parameters, we repeat the same calculation for various (H_0, T_s) combinations, guided by observational constraints (1, 32, 34) and for three different p_α values. For each (H_0, T_s) combination, we search for a γ that can lead to the hemispheric symmetry breaking, and meanwhile, guarantees that the

global mean tidal heating rate wouldn't exceed the global mean heat loss to space[†]. The combinations that allow us to find such a γ are marked by the white color in Fig. 4. The three panels show results for $p_\alpha = -1.5, -2, -2.5$, respectively.

As $|p_\alpha|$ increases, the symmetry breaking regime gradually widens, as does the range of γ that can trigger the symmetry breaking. This is unsurprising because a greater $|p_\alpha|$ can enhance the growth of ice topography, which is one of the two necessary elements for symmetry breaking to happen.

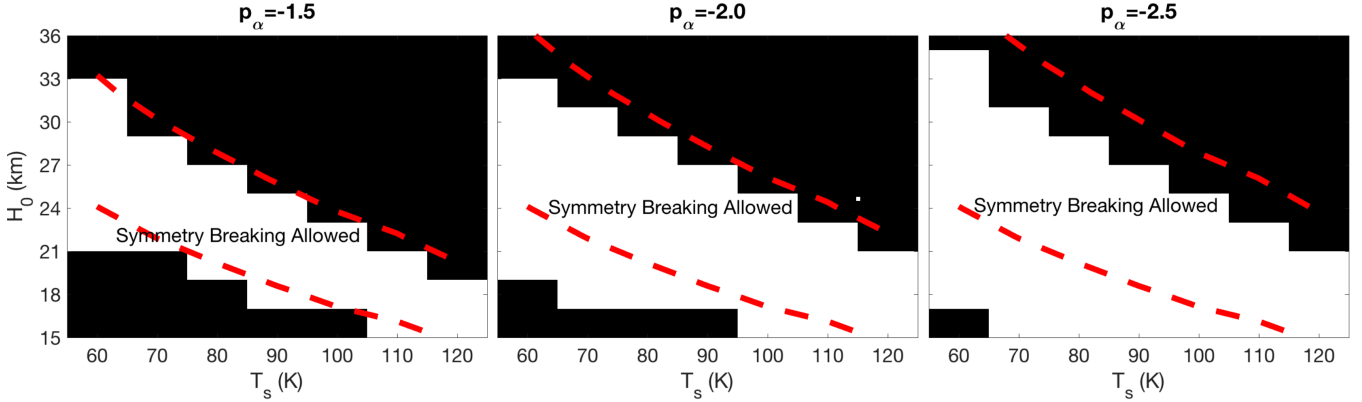


Fig. 4. Diagram showing the combinations that permit symmetry breaking of the global mean ice shell thickness H_0 and the surface temperature T_s . White denotes the parameter regimes that allow us to find a γ that can lead to symmetry breaking. Red curves show the symmetry breaking criteria given by Eq. (2) with $\beta = 1, \tau_F/\tau_T = 1$.

From Fig. 4, one can clearly see that, for any given p_α and T_s , symmetry breaking can only occur in a specific range of H_0 . With an ice thickness beyond the upper bound (no symmetry breaking regimes are found for $H_0 \leq 36$ km), symmetry breaking does not occur because the ice flow becomes too efficient[‡] to maintain any topography. With ice thickness below the lower bound, the ice flow is too weak to maintain a crack-free H_{eq} in absence of perturbations. According to the stability analysis shown in the supplementary material, the symmetry breaking regime should satisfy the following criteria:

$$\frac{\beta(\tau_F/\tau_T)}{4} < \frac{\tau_F}{\tau_Q} < -p_\alpha(\tau_F/\tau_T)(\beta/2 + 1) - 1 \quad [2]$$

Here, τ_F, τ_T, τ_Q are the timescales for heat conduction, tidal heating, and ice flow that significantly change the planetary-scale ice topography, and β is the percentage variation of \mathcal{T} about the mean across different latitudes (see supplementary material for definitions). As shown by red dashed curves in Fig. 4, Eq. 2 predicts the location of the symmetry breaking regime in the (T_s, H_0) parameter space well, especially for $p_\alpha = -1.5$. For greater $|p_\alpha|$, τ_F/τ_T becomes significantly smaller than 1 when symmetry breaking occurs; therefore, the actual symmetry breaking regime is more on the low side of H_0 , compared to the prediction given by Eq. 2.

For such a symmetry breaking regime to exist, the upper bound of Eq. (2) has to be larger than the lower bound, which leads to an additional necessary condition for ice shell symmetry breaking,

$$\frac{\tau_F}{\tau_T} > \frac{1}{-p_\alpha(\beta/2 + 1) - \beta/4}. \quad [3]$$

This sets a lower bound for the percentage of heat loss that is compensated by the tidal heating in the ice shell. For the example, as we show in the results, this condition would be satisfied if the ice dissipation rate is enhanced by a γ factor greater than 14.8, which could be possible given that the Maxwell body rheology used here could significantly underestimate the dissipation rate (28, 29).

The ice shell symmetry breaking criteria (Eq. 2 and Eq. 3) can be applied to other icy moons, if their orbital parameters and physical characteristics are known. For icy moons around Jupiter and Saturn whose

[†]This leaves room for other heat sources.

[‡]As mentioned in the model overview and shown in the supplementary material, ice flow becomes more (less) efficient when ice shell is thick (thin).

ice shell is a major heat producer (i.e., Eq. 3 is satisfied), symmetry breaking would occur at roughly the same H_0 , regardless of other parameters. Substituting the definitions of $\tau_{\mathcal{F}}$ and $\tau_{\mathcal{Q}}$ into Eq. (2) and noticing that both the lower and upper bound of that inequality are of $O(1)$, we get

$$\frac{\tau_{\mathcal{F}}}{\tau_{\mathcal{Q}}} \propto \frac{H_0^5}{(a^2/g)(\bar{\eta} \log(T_m/T_s))} \sim O(10^{-8}), \quad [4]$$

where g and a are the surface gravity and radius of Enceladus, and $\bar{\eta}$ is a weighted average viscosity across the ice shell, whose definition is given in the supplementary material. The 10^{-8} on the right comes from a combination of physical constants, including fusion energy, thermal conductivity, and density of the ice. The fact that $\tau_{\mathcal{F}}/\tau_{\mathcal{Q}}$ is proportional to the fifth power of H_0 implies the symmetry breaking regime is always centered around $H_0 \sim 10$ -30 km. Even if the radius of the moon is enlarged by 10 times (while keeping the bulk density unchanged), a^2/g would increase by a factor of 10, and the symmetry breaking permitting H_0 would only change by a factor of $(10)^{1/5} \sim 1.6$. The Galilean satellites are warmer than Saturnian satellites by about 30K, and the associated impact on H_0 is no larger than a factor of 2 as well. This leads to an even simpler empirical rule for the mechanism proposed here: ice shell symmetry breaking would only occur on Galilean and Saturnian icy moons whose ice shell thickness is around 10-30 km.

Our calculation assumes the ice shell is conductive. However, besides Enceladus, the only place inside our solar system that satisfies this assumption is Europa; other icy moons (such as Titan, Ganymede, Callisto) have an ice shell that is too thick (35–38) for ice convection to be triggered (39). Repeating the same calculation for Europa, we found symmetry breaking could only occur when the ice shell thickness is 20-26 km, assuming the mean surface temperature is around 100 K (40) and $p_{\alpha} = -1.5$. Based on magnetic conduction, Europa’s ice shell thickness is constrained to be below 15 km (41), indicating that Europa could have narrowly missed the symmetry-breaking regime. However, the estimation of Europa’s ice shell thickness is not yet conclusive (35, 42, 43), so more studies are needed to improve the thickness estimation and the symmetry breaking criteria.

To make the problem analytically approachable, we made many simplifications and assumptions, which could have an impact on the symmetry breaking regime. For example, when considering the tidal heating generated in an inhomogeneous ice shell, we multiply $\mathcal{T}_0^{\text{mem}}$ by a factor of $(H/H_0)^{p_{\alpha}}$ rather than solve the thin shell ODE with variable coefficients. As a result, we ignore the fact that small-scale perturbations would be suppressed by the greater bending rigidity associated with it. Taking this into consideration would lead to a stronger scale selectivity. In addition, the slow circulation in the slush zone at the ocean-ice interface can also help damp the small-scale topographies, widening the symmetry breaking regime. We also ignore the decrease of surface temperature toward the poles, as the role played by this factor is less clear and will be explored in future work.

Other ignored mechanisms, such as ocean circulation, surface snow cover, dynamics of ice convection, and non-Newtonian ice rheology, could also affect the parameter regime where this mechanism works and the rate at which hemispheric asymmetry grows. Particularly, tidal heating from the core is found to be necessary to counterbalance the heat conduction to space, as heating generated in the ice shell alone is not enough, given our current understanding of ice dynamics (26, 27). The heating generated in the core is carried upward by eddies, convection plumes, and large-scale circulation in the ocean. It is possible that some of these processes could respond to changes in ice topography and form a feedback loop, as suggested by (44). We speculate that freezing (melting) at the ocean-ice interface may be able to reduce (increase) the local salinity and drive an upwelling (sinking) motion there, which in turn enhances (reduces) the upward heat transport from the core and leads to further freezing (melting). Feedback like this can be accounted for in our framework by a greater p_{α} factor. Processes that are not directly affected by the ice topography are represented by the balancing term \mathcal{B} . Our work assumes a globally uniform profile of \mathcal{B} , but it is highly possible that \mathcal{B} is concentrated in a few hot spots (30). If that is true, the equilibrium state h'_{eq} would change, which would in turn affect the growing mode structure and its growth rate. Even a tiny hemispheric asymmetry in \mathcal{B} would help determine the direction of symmetry breaking, and it could significantly affect the parameter regime where symmetry breaking could happen.

Concluding remarks

Our work takes an idealized framework to demonstrate the feasibility of spontaneous hemispheric symmetry breaking. Over billions of years, Enceladus could have gone through large eccentricity variations (45–47), leading to secular melting/freezing over time. As the ice shell thickness varies, it seems unavoidable that Enceladus would pass through the symmetry breaking regime shown in Fig. 4. When Enceladus gets into the symmetry breaking regime, hemispheric asymmetry would accumulate; when it gets out, hemispheric asymmetry would gradually decay. Before the historical orbital record is obtained, understanding the stochastic dynamics of this system would shed light on how much hemispheric asymmetry of Enceladus can be developed through the mechanism proposed here.

ACKNOWLEDGMENTS. Most of this work was carried out during the 2019 Geophysical Fluid Dynamics Summer School at Woods Hole. We thank the GFD faculty for organizing the program and the Woods Hole Oceanographic Institution for hosting it. During the review process, the two anonymous reviewers gave us extremely helpful comments, which we deeply appreciate. We also thank Prof. Geoff Vasil and Prof. Ming Cai for helpful discussions.

1. D Hemingway, L Iess, R Tadjeddine, G Tobie, The Interior of Enceladus in *Enceladus and the Icy Moons of Saturn*. (The University of Arizona Press), (2018).
2. Roberts, James H, Nimmo, Francis, Tidal heating and the long-term stability of a subsurface ocean on Enceladus. *Icarus* **194**, 675–689 (2008).
3. CJ Hansen, et al., Enceladus' Water Vapor Plume. *Science* **311**, 1422–1425 (2006).
4. JR Spencer, F Nimmo, Enceladus: An Active Ice World in the Saturn System. *Annu. Rev. Earth Planet. Sci.* **41**, 693–717 (2013).
5. JH Waite, et al., Cassini Ion and Neutral Mass Spectrometer: Enceladus Plume Composition and Structure. *Science* **311**, 1419–1422 (2006).
6. JH Waite, et al., Cassini finds molecular hydrogen in the Enceladus plume: Evidence for hydrothermal processes. *Science* **356**, 155–159 (2017).
7. CJA Howett, JR Spencer, J Pearl, M Segura, High heat flow from Enceladus' south polar region measured using 10-600 cm-1 Cassini/CIRS data. *J. Geophys. Res.* **116**, 189 (2011).
8. JR Spencer, et al., Enceladus Heat Flow from High Spatial Resolution Thermal Emission Observations. *Eur. Planet. Sci. Congr.* **8**, EPSC2013–840 (2013).
9. L Iess, et al., The Gravity Field and Interior Structure of Enceladus. *Science* **344**, 78–80 (2014).
10. C Porco, et al., Enceladus' jets: particle characteristics, surface source locations, temporal variability, and correlations with thermal hot spots in *Lunar and Planetary Science Conference*. Vol. 38, p. 2310 (2007).
11. Chen, E M A, Nimmo, F, Obliquity tides do not significantly heat Enceladus. *Icarus* **214**, 779–781 (2011).
12. RM Baland, M Yseboodt, T Van Hoolst, The obliquity of Enceladus. *Icarus* **268**, 12–31 (2016).
13. L Han, AP Showman, Coupled convection and tidal dissipation in Europa's ice shell. *Icarus* **207**, 834–844 (2010).
14. L Han, G Tobie, AP Showman, The impact of a weak south pole on thermal convection in enceladus' ice shell. *Icarus* **218**, 320–330 (2012).
15. M Behounkova, G Tobie, G Choblet, O Cadek, Tidally-induced melting events as the origin of south-pole activity on Enceladus. *Icarus* **219**, 655–664 (2012).
16. Rozel, A, Besserer, J, Golabek, G, J, Kaplan, M, Tackley, P, J, Self-consistent generation of single-plume state for Enceladus using non-Newtonian rheology. *J. Geophys. Res. Planets* **119**, 416–439 (2014).
17. F Nimmo, RT Pappalardo, Diapir-induced reorientation of Saturn's moon Enceladus. *Nature* **441**, 614–616 (2006).
18. DR Stegman, J Freeman, DA May, Origin of ice diapirism, true polar wander, subsurface ocean, and tiger stripes of Enceladus driven by compositional convection. *Icarus* **202**, 669–680 (2009).
19. R Tadjeddine, et al., True polar wander of Enceladus from topographic data. *Icarus* **295**, 46–60 (2017).
20. DJ Hemingway, ML Rudolph, M Manga, Cascading parallel fractures on Enceladus. *Nat. Astron.* **3**, 1–6 (2019).
21. GW Ojakangas, DJ Stevenson, Thermal state of an ice shell on Europa. *Icarus* **81**, 220–241 (1989).
22. EMA Chen, F Nimmo, GA Glatzmaier, Tidal heating in icy satellite oceans. *Icarus* **229**, 11–30 (2014).
23. I Matsuyama, M Beuthe, HCFC Hay, F Nimmo, S Kamata, Ocean tidal heating in icy satellites with solid shells. *Icarus* **312**, 208–230 (2018).
24. M Beuthe, Spatial patterns of tidal heating. *Icarus* **223**, 308–329 (2013).
25. M Beuthe, Enceladus's crust as a non-uniform thin shell: I tidal deformations. *Icarus* **302**, 145–174 (2018).
26. M Beuthe, Enceladus's crust as a non-uniform thin shell: II tidal dissipation. *Icarus* **332**, 66–91 (2019).
27. DJ Hemingway, T Mittal, Enceladus's ice shell structure as a window on internal heat production. *Icarus* **332**, 111–131 (2019).
28. C McCarthy, RF Cooper, Tidal dissipation in creeping ice and the thermal evolution of Europa. *Earth Planet. Sci. Lett.* **443**, 185–194 (2016).
29. JP Renaud, WG Henning, Increased Tidal Dissipation Using Advanced Rheological Models: Implications for Io and Tidally Active Exoplanets. *Astrophys. J.* **857**, 98 (2018).
30. G Choblet, et al., Powering prolonged hydrothermal activity inside Enceladus. *Nat. Astron.* **1**, 841–847 (2017).
31. HCFC Hay, I Matsuyama, Nonlinear tidal dissipation in the subsurface oceans of Enceladus and other icy satellites. *Icarus* **319**, 68–85 (2019).
32. O Čadek, et al., Enceladus's internal ocean and ice shell constrained from Cassini gravity, shape, and libration data. *Geophys. Res. Lett.* **43**, 5653–5660 (2016).
33. M Beuthe, Crustal control of dissipative ocean tides in Enceladus and other icy moons. *Icarus* **280**, 278–299 (2016).
34. M Beuthe, A Rivoldini, A Trinh, Enceladus's and Dione's floating ice shells supported by minimum stress isostasy. *Geophys. Res. Lett.* **43**, 10,088–10,096 (2016).
35. PM Schenk, Thickness constraints on the icy shells of the galilean satellites from a comparison of crater shapes. *Nature* **417**, 419–421 (2002).
36. OL Kuskov, VA Kronrod, Models of the Internal Structure of Callisto. *Sol. Syst. Res.* **39**, 283–301 (2005).
37. D Hemingway, F Nimmo, H Zebker, L Iess, A rigid and weathered ice shell on Titan. *Nature* **500**, 550–552 (2013).
38. T Spohn, *Treatise on Geophysics, Volume 10: Planets and Moons*. (Newnes) Vol. 10, (2010).
39. WB McKinnon, On convection in ice I shells of outer Solar System bodies, with detailed application to Callisto. *Icarus* **183**, 435–450 (2006).
40. LA McFadden, P Weissman, T Johnson, Encyclopedia of the solar system, by lucy-ann mcfadden, paul r. weissman, and torrence v. johnson. *Sky Telesc.* **114**, 74 (2007).
41. K Hand, C Chyba, Empirical constraints on the salinity of the european ocean and implications for a thin ice shell. *Icarus* **189**, 424–438 (2007).
42. G Tobie, G Choblet, C Sotin, Tidally heated convection: Constraints on Europa's ice shell thickness. *JOURNAL OF GEOPHYSICAL RESEARCH-ATMOSPHERES* **108**, 219 (2003).
43. F Nimmo, B Giese, RT Pappalardo, Estimates of Europa's ice shell thickness from elastically-supported topography. *Geophys. Res. Lett.* **30**, n/a–n/a (2003).
44. Y Ashkenazy, R Sayag, E Tziperman, Dynamics of the global meridional ice flow of Europa's icy shell. *Nat. Astron.* **2**, 43–49 (2018).
45. J Meyer, J Wisdom, Tidal heating in Enceladus. *Icarus* **188**, 535–539 (2007).
46. C Yoder, Tidal friction and enceladus' anomalous surface. *Eos* **62**, 939 (1981).
47. GW Ojakangas, DJ Stevenson, Episodic volcanism of tidally heated satellites with application to Io. *Icarus* **66**, 341–358 (1986).